

# Production of Large Rapidity Gap Events in $ep$ Interactions at HERA \*

Halina Abramowicz  
School of Physics, Tel-Aviv University  
Representing the ZEUS Collaboration

## Abstract

This is a short review of the properties of electron proton interactions characterized by the presence of large rapidity gaps (LRG) in the measured hadronic final state as obtained by the ZEUS Collaboration at the HERA Collider. In the deep inelastic neutral current  $ep$  interactions, the factorization properties of the LRG events interpreted as due to the diffractive dissociation of the virtual photon are compatible with expectations from the Regge phenomenology of soft interactions. The measurement of deep inelastic scattering combined with results from photoproduction of high  $p_T$  jets are successfully interpreted in terms of a factorizable Pomeron consisting of quarks and with a substantial contribution of a gluonic component. The first hints of a more complicated nature of the Pomeron are observed in the deep inelastic exclusive  $\rho^0$  production, where a strong increase of the production cross section with energy is observed relative to the measurements of the NMC Collaboration at lower energy.

---

\*Talk given at the VIth Blois Workshop on Frontiers in Strong Interactions, Blois, France, June 20–24, 1995

# 1 Introduction

The study of  $ep$  interactions at the HERA collider, where 26.7 GeV electrons collide with 820 GeV protons, has led to the observation of many interesting effects, with highlights such as the strong rise of the proton structure function  $F_2$  in the region of low Bjorken  $x$  even at moderate momentum transfers  $Q^2 \sim 10$  GeV [1, 2] and the production of large rapidity gap (LRG) events in the deep inelastic neutral current interactions [3, 4] and in high  $p_T$  jet photoproduction [5, 6]. Particles produced in inelastic, non diffractive hadron hadron interactions, are known to populate a cylindrical phase space (with limited  $p_T$ ) available for their production, with three characteristic domains: the two fragmentation regions corresponding to the initial beam particles and the central region. A similar picture emerges in  $ep$  interactions [7] when viewed from the  $\gamma^*p$  frame after removing the scattered electron. On the other hand particles originating from a diffractively excited  $\gamma^*$  will only populate the photon fragmentation region and lead to a large rapidity gap (LRG) extending through (part of) the central and proton fragmentation regions.

The initial study of the LRG events observed in NC DIS interactions at HERA [3, 4, 8] led to the conclusion that: (1) the  $Q^2$  dependence was consistent with originating from a leading twist effect, (2) the ratio of LRG events to all the events was almost constant with  $W$ , (3) a small fraction of about 3% of the LRG events had large  $p_T$  jets in the final state, thus leading to a picture of predominantly soft hadronic configurations. The emerging picture was consistent with the assumption of a DIS scattering on a quark originating from a Pomeron like object, in good agreement with models such as that of Ingelman-Schlein [9], Donnachie–Landshoff [10] or of Nikolaev-Zakharov [11].

## 2 Large Rapidity Gap Events in the ZEUS detector

The ZEUS detector [12] consists of the vertex detector, the central tracking chamber, the high resolution uranium/scintillator calorimeter (CAL) and a muon spectrometer consisting in turn of an iron backing calorimeter sandwiched between precision muon chambers. In the forward (defined along the momentum vector of the incoming proton) and rear (defined by the momentum vector of the incoming electron) directions the tracking is supplemented by the forward and rear tracking chambers. The maximal rapidity acceptance is given by the CAL and extends from 4.2 to -3.8 units of pseudorapidity  $\eta$  ( $\eta = -\ln \tan \frac{\theta}{2}$  with  $\theta$  the polar angle measured with respect to the proton direction).

A leading proton spectrometer, LPS, consisting of a chain of roman pots surrounding the beam pipe is located in the forward region to tag and measure diffractive photon dissociation reactions. A forward neutron calorimeter, FNC, has been designed to tag high energy neutrons originating from the  $ep$  interactions.

The luminosity is determined by measuring the integrated Bethe-Heitler photon spectrum ( $ep \rightarrow ep\gamma$ ), measured in the luminosity gamma detector located downstream of the electron beam.

The  $ep$  interactions are classified as NC DIS if the scattered electron is detected in the CAL and as photoproduction otherwise. The separation occurs typically for photon virtualities of  $Q^2 = 4$  GeV<sup>2</sup>.

In this presentation the operational definition of diffractive events is adopted following Bjorken [13]: ” A diffractive process occurs if and only if there is a large rapidity gap in the produced particle phase space which is not exponentially suppressed.” In the HERA regime diffractive photon dissociation can be tagged by a presence of a LRG for masses up to about 20 GeV which can

be fully contained in the acceptance region of the central detector. To select large rapidity

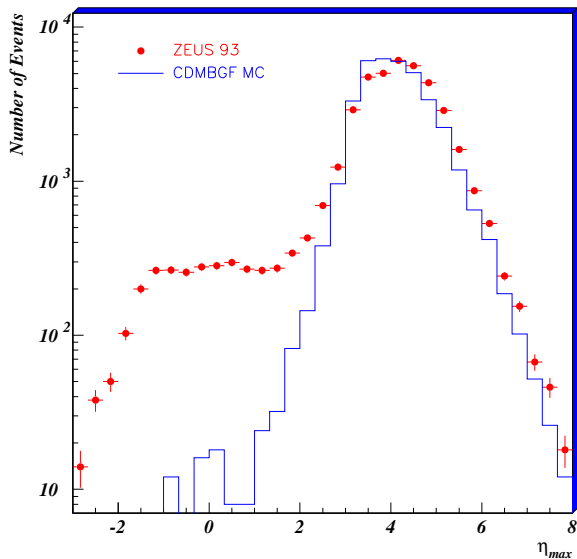


Figure 1: *Distribution of  $\eta_{\max}$  as defined in the text for DIS NC events in the data (dots) and in the MC. (histogram)*

gap events we define for each event  $\eta_{\max}$  as the  $\eta$  of an energy deposit in the detector above 400 MeV closest to the proton direction. The distribution of  $\eta_{\max}$  for selected DIS NC events with  $Q^2 > 8 \text{ GeV}^2$  is presented in figure 1 and compared with a DIS Monte Carlo (MC) based on the Color Dipole Model (ARIADNE [14]) for the production of the hadronic final state. A clear excess of events with large rapidity gaps is observed, in the region of  $\eta_{\max} < 2$  which corresponds to an effective rapidity gap of more than 2 units of  $\eta$  in the detector and possibly more than 5 units of  $\eta$  relative to the initial proton. In the MC the LRG events are strongly suppressed in this region.

### 3 Diffractive Deep Inelastic Scattering

The LRG events can be described by the following set of inclusive variables: the negative of the four momentum transfer squared between the incoming and the scattered electron  $-Q^2$ ; the fraction of the proton momentum carried by the struck quark determined by Bjorken  $x$ ; the invariant mass of the hadronic final state  $W$  equal to the center of mass energy of the  $\gamma^*p$  system; the square of the momentum transfer,  $t$ , between the initial and final proton; the invariant mass of the hadrons excluding the final state proton,  $M_X$ ; and finally the fraction of the proton momentum carried by the (generic) pomeron  $x_{\mathcal{P}}$ . It is customary to introduce a variable which denotes the fraction of the pomeron momentum carried by the struck quark,  $\beta = x/x_{\mathcal{P}}$ .

Assuming  $t \simeq 0$  and neglecting the mass of the proton

$$x_{\mathcal{P}} = \frac{Q^2 + M_X^2}{Q^2 + W^2}, \quad \beta = \frac{Q^2}{Q^2 + M_X^2}. \quad (1)$$

To study the factorization properties of LRG events it is convenient to rewrite the differential DIS  $ep$  cross section as a function of  $Q^2$ ,  $\beta$  and  $x_{\mathcal{P}}$ ,

$$\frac{d^3\sigma}{d\beta dQ^2 dx_{\mathcal{P}}} = \frac{2\pi\alpha^2}{\beta Q^2} [1 + (1 - y)^2] F_2^{D(3)}(\beta, Q^2, x_{\mathcal{P}}), \quad (2)$$

where  $y = \frac{Q^2}{xs}$  with  $s$  the  $ep$  center of mass energy squared and  $F_2^{D(3)}$  denotes the contribution of LRG events with a given  $x_P$  integrated over  $t$  to the  $F_2$  structure function of the proton for a given  $Q^2$  and  $x = \beta x_P$ . For simplicity the contribution from the  $F_L$  structure function has been omitted in the above formula.

Should the mechanism of diffractive production in DIS be similar to that ruling the soft hadron hadron interactions, the  $F_2^{D(3)}$  is expected to factorize into a flux factor  $f_P$  and the structure function of the pomeron  $F_2^P(\beta, Q^2)$ :  $F_2^{D(3)} = f_P(x_P) \times F_2^P(\beta, Q^2)$ . Moreover if the LRG events are induced by the  $P$  trajectory of the Regge phenomenology,  $\alpha_P(t) = 1 + \epsilon + \alpha' t$  with  $\epsilon = 0.08$  [15] and  $\alpha' = 0.25 \text{ GeV}^{-2}$ , the  $x_P$  dependence of the flux integrated over  $t$  is expected to be

$$f_P(x_P) \sim \frac{1}{x_P^{1.16}} \cdot x_P^{0.06 \div 0.04}.$$

The term of  $x_P^{0.06 \div 0.04}$  comes from the slope of the  $P$  trajectory and the variation depends on the assumed  $t$  dependence of the diffractive peak ( $\sim e^{Bt}$  with  $B = 4.5 \div 8 \text{ GeV}^{-2}$ ). The structure function  $F_2^P$  would then depend on the partonic structure of the pomeron. This is the essence of the Ingelman–Schlein [9] and Donnachie–Landshoff [10] models for diffraction in DIS. Note that the separation of  $F_2^{D(3)}$  into a flux term and  $F_2^P$  is not unique since the normalization of  $F_2^P$  is not known.

In the Nikolaev–Zakharov model [11] the pomeron is modelled by a two gluon exchange with an addition of multi–gluon exchanges parameterized by the triple Regge formula. This leads to an explicit factorization breaking, although the effect is small. In the model of Capella et al. [16] the flux of the  $P$  is determined by the intercept of the bare pomeron and the structure function of the  $P$  is related to that of the deuterium.

The results reported here correspond to an integrated luminosity of  $0.54 \text{ pb}^{-1}$  collected during the 1993 running period. The selection of events on the basis of the  $\eta_{\text{max}} \leq 1.5$  cut leads to a very clean sample of LRG events, yet it restricts the analysis to relatively small masses (typically  $M_X \lesssim 10 \text{ GeV}$ ). The efficiency to select larger masses can be improved at the expense of an increased background from the non-diffractive DIS events. In the analysis presented here the LRG events were selected requiring  $\eta_{\text{max}} < 2.5$  and  $\cos \theta_h = \sum_i p_{zi} / \sum_i \vec{p}_i < 0.75$ , where the sum runs over all calorimeter clusters assigned to the hadronic final state. The latter cut allows to separate large mass diffractive events which do not exhibit a LRG in the calorimeter from non-diffractive events in which due to the fragmentation of the proton system the hadronic energy measured in the forward calorimeter is large and thus  $\cos \theta_h \simeq 1$ . The remaining background from non-diffractive events is estimated with the DIS MC based on the Color Dipole Model including boson gluon fusion diagrams [14] and subtracted. The contribution from double diffractive dissociation is estimated to be  $15 \pm 10\%$  and is not subtracted. It is assumed to be independent of  $x_P$ . Only events with  $0.08 < y < 0.5$  were used in the analysis. The upper cut is applied in order to limit the contribution from the unknown longitudinal structure function for the LRG component. The results of the  $F_2^{D(3)}$  determination are presented in bins of  $\beta$  and  $Q^2$  as a function of  $x_P$  in figure 2. The data can be well represented by a fit of the form

$$F_2^{D(3)}(\beta, Q^2, x_P) = \left( \frac{1}{x_P} \right)^a C_{\beta, Q^2},$$

where  $a$  is kept fixed for all  $\beta, Q^2$  bins and  $C$  is a constant allowed to vary from bin to bin. The result of the fit yields

$$a = 1.30 \pm 0.08(\text{stat.})_{-0.14}^{+0.08}(\text{syst.})$$

ZEUS 1993

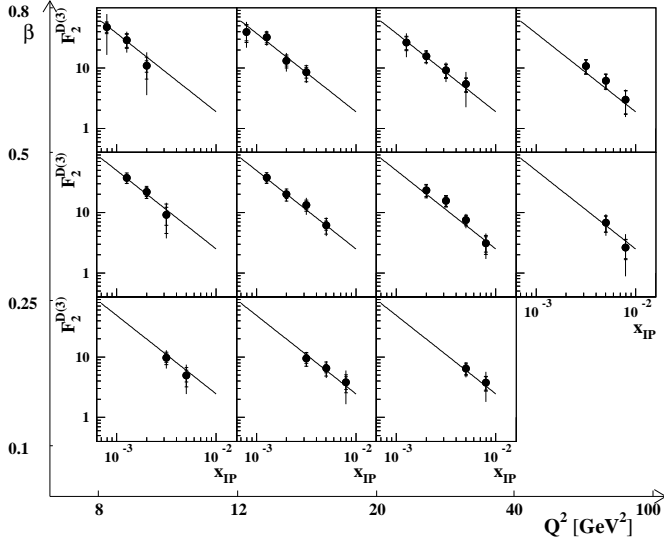


Figure 2:  $F_2^{D(3)}(\beta, Q^2, x_{\mathcal{P}})$  as a function of  $x_{\mathcal{P}}$  for fixed  $\beta$  and  $Q^2$ , compared to the parameterization discussed in the text. The statistical and systematic errors are shown separately as well as the total error. Note that the data include an estimated 15% contribution due to double dissociation. The overall normalization uncertainty of 3.5% due to the luminosity uncertainty is not included.

All the data are well described by

$$F_2^{D(3)}(\beta, Q^2, x_{\mathcal{P}}) = 0.018 \left( \frac{1}{x_{\mathcal{P}}} \right)^{1.30} \left( \beta(1 - \beta) + \frac{0.57}{2}(1 - \beta)^2 \right),$$

with no  $Q^2$  dependence. The result of the fit is presented in figure 2. It is within errors compatible with diffractive production being driven by the soft  $\mathcal{P}$ . We define  $\tilde{F}_2^D(\beta, Q^2)$  as

$$\tilde{F}_2^D(\beta, Q^2) = \int_{6.3 \cdot 10^{-4}}^{10^{-2}} F_2^{D(3)}(\beta, Q^2, x_{\mathcal{P}}) dx_{\mathcal{P}}$$

The  $\beta$  dependence for fixed  $Q^2$  values and the  $Q^2$  dependence for fixed  $\beta$  values of  $\tilde{F}_2^D(\beta, Q^2)$

ZEUS 1993

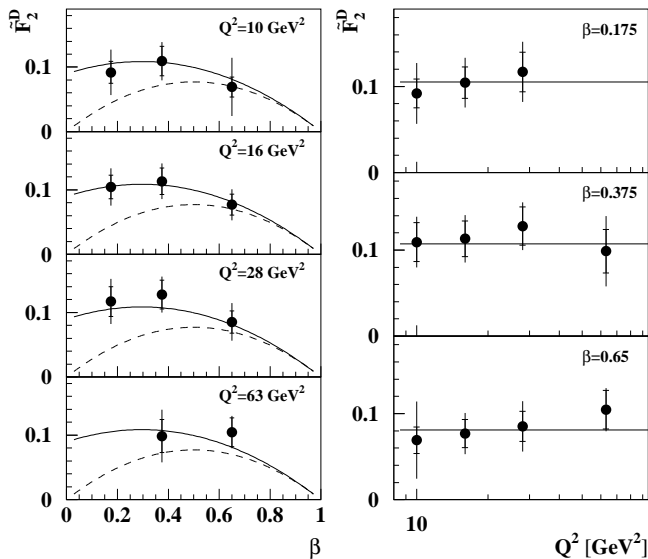


Figure 3:  $\tilde{F}_2^D(\beta, Q^2)$  as a function of  $\beta$  for fixed  $Q^2$  and as a function of  $Q^2$  for fixed  $\beta$ . The full line indicates the parameterization discussed in the text. The  $\beta(1 - \beta)$  contribution is indicated by the dashed line.

is presented in figure 3. The  $\beta$  distribution is compared to the form  $\beta(1 - \beta)$  expected in the splitting of the  $\mathcal{P}$  into a  $q\bar{q}$  pair. A clear excess of low  $\beta$  events is observed. Within

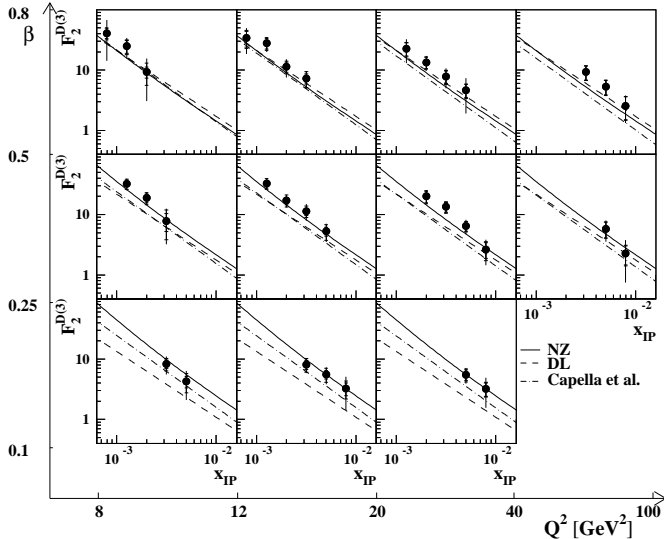


Figure 4:  $F_2^{D(3)}$  compared to various models discussed in the text. The estimated 15% contribution due to double dissociation has been subtracted. The overall normalization uncertainty of 3.5% due to the luminosity and 10% due to the subtraction of the double dissociation background is not included in the error bars.

the statistical and systematic errors the result is compatible with no  $Q^2$  dependence even at the largest value of  $\beta$ . The comparison with the various models discussed above presented in figure 4 shows that the models of Nikolaev-Zakharov and of Capella et al. give the best description of the data. The model of Donnachie–Landshoff reproduces the data well in the region of  $\beta > 0.25$  where the contribution of the  $f$  trajectory is negligible. The original model of Ingelman–Schlein (not shown), which assumes that quarks saturate the momentum sum rule for the  $\mathbb{P}$  overestimates the cross section by a large factor.

It should be noted that the  $F_2^{D(3)}$  dependence on  $x_{\mathbb{P}}$ ,  $\beta$  and  $Q^2$  is also well reproduced by the model of Buchmueller and Hebecker [17] which does not use the concept of the Pomeron, but rather describes the production of LRG through one gluon exchange with a non-perturbative color cancellation induced by wee partons.

## 4 Diffractive jet production in hard photoproduction

The first observation of the partonic substructure of diffractive proton dissociation was reported by the UA8 experiment [18] in two jet production associated with a tagged leading proton. An analogous measurement was performed by ZEUS [5, 19] where large  $p_T$  jet production was studied for photoproduction events with a LRG,  $\eta_{\max} < 1.8$ . The inclusive cross section  $d\sigma/d\eta^{jet}$  was determined in the energy range  $135 \lesssim W \lesssim 280$  GeV for  $-1 < \eta^{jet} < 1$ , requiring the transverse jet energy  $E_T > 8$  GeV. The cross section was then compared with expectations of a model in which jet production with a LRG in the forward region is due to a hard scattering between the partons of the pomeron and the photon. Both the direct photon and resolved photon contribution were taken into account, with the  $\gamma$  structure function as given by the GS–HO parameterization [20]. The flux of the  $\mathbb{P}$  was assumed to be given by the Donnachie–Landshoff parameterization [21] and the pomeron was assumed to consist of either only quarks or only gluons, soft or hard, in each case saturating the momentum sum rule. The results of the comparison are shown in figure 5. Also shown is the contribution expected from fluctuations of the hadronic final state in non-diffractive jet photoproduction. The excess of events with LRG is best described by a pomeron consisting of hard gluons. It is clear though that a combination of gluons and quarks would also reproduce the cross section. The photoproduction data alone cannot be used to decompose the content of the pomeron without further assumptions about

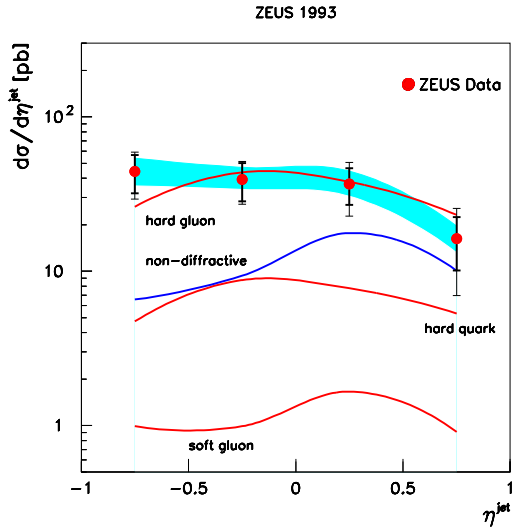


Figure 5: Measured differential ep cross section  $d\sigma/d\eta^{jet}(\eta_{\max} < 1.8)$  for inclusive jet production. The measurements are not corrected for the contributions from non-diffractive processes and double dissociation. The inner error bars represent the statistical errors of the data, and the total error bars show the statistical and systematic errors added in quadrature. The shaded band displays the uncertainty due to the energy scale of the jets, not included in the error bars.

the flux of the  $\mathbb{P}$  and the associated momentum sum rule.

## 5 Partonic Content of the Pomeron

The DIS data on the  $F_2^{D(3)}$  structure function, sensitive to the quark content, and the jet photoproduction cross section, sensitive to both the quark and gluon content, can be combined to estimate the percentage of the  $\mathbb{P}$  momentum carried by the quarks and the gluons. This is done in the following way. The pomeron flux is assumed to be the same in photoproduction and in DIS and given by the Donnachie–Landshoff parameterization. The shape of the quark distribution is taken as determined from the DIS measurement and is normalized to one. The gluon distribution is assumed to be of the form  $\beta(1-\beta)$  and also normalized to one. Then both the DIS and the jet photoproduction cross sections are calculated assuming that the gluons carry  $c_g$  fraction of the pomeron momentum, the rest being carried by the quarks. For each  $c_g$  the overall normalization  $\Sigma_{\mathbb{P}}$  needed to reproduce the measured cross section is determined separately for the two reactions. The results are presented in figure 6. The region where the  $\Sigma_{\mathbb{P}}$

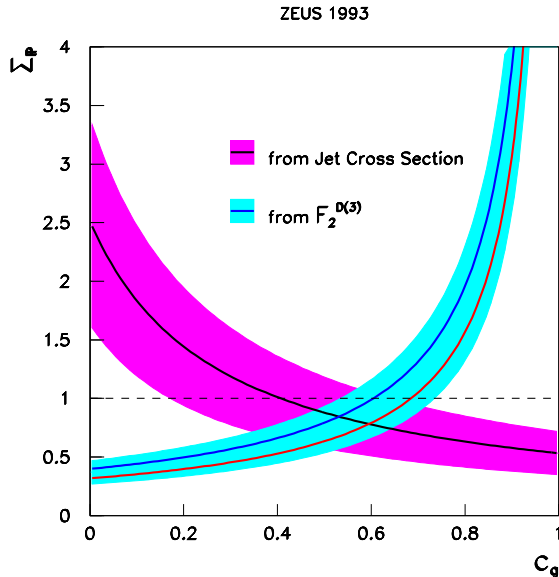


Figure 6: The overall normalization coefficient  $\Sigma_{\mathbb{P}}$  required to describe the jet cross section and the  $F_2^{D(3)}$  measurement, assuming a factorizable pomeron consisting of hard gluons carrying a  $c_g$  fraction of its momentum and of quarks carrying a  $1 - c_g$  fraction of its momentum.

is the same for both reactions determines the gluon content of the pomeron. This happens for  $0.3 < c_g < 0.8$ , where the range is determined by the statistical and systematic uncertainties on the cross section measurements. Note that this result does not depend on the assumed pomeron flux, nor on the contribution of the proton dissociation. It is also independent of any assumption on the validity of the momentum sum rule for the pomeron. The conclusion is thus that the gluon content of the pomeron is substantial.

The same conclusion can be drawn from the lack of  $Q^2$  evolution of  $F_2^{\mathbb{P}}$  at large  $\beta$ , assuming that the DGLAP evolution equation applies to the pomeron [22]. Since, as is the case for the proton, parton radiation leads to the depletion of quarks at large  $\beta$  ( $x$  in the proton case), the only way to compensate this depletion is by adding quarks from another source - gluon radiation of quarks. These gluons have to be then at  $\beta \rightarrow 1$ . The numerical estimate of this effect can be found in [23].

## 6 Vector meson production in DIS

Another example of a reaction which leads to LRG in the final states of electroproduction is the exclusive production of vector mesons (see contribution by J. Whitmore to this conference) such as  $ep \rightarrow e\rho p$ . The previously existing data from photoproduction [24] and electroproduction [25] were compatible with expectations based on the Pomeron phenomenology. In a model proposed by Donnachie and Landshoff [26] the  $\mathbb{P}$  consists of two non-perturbative gluons and the large  $Q^2$   $\rho$  production cross section is predicted to have the following form:

$$\sigma(\gamma^*p \rightarrow \rho^0 p) \sim \frac{(xg(x, Q^2))^2}{Q^6},$$

where the  $x$  dependence of the  $xg(x, Q^2)$  is determined by the intercept of the soft  $\mathbb{P}$ . Thus the  $\rho^0$  production cross section is expected to rise only slowly with  $W$ ,  $\sigma(\gamma^*p \rightarrow \rho^0 p) \sim W^{0.32}$ . This expectation is to be contrasted with the recent calculation of Brodsky et al. [27] which

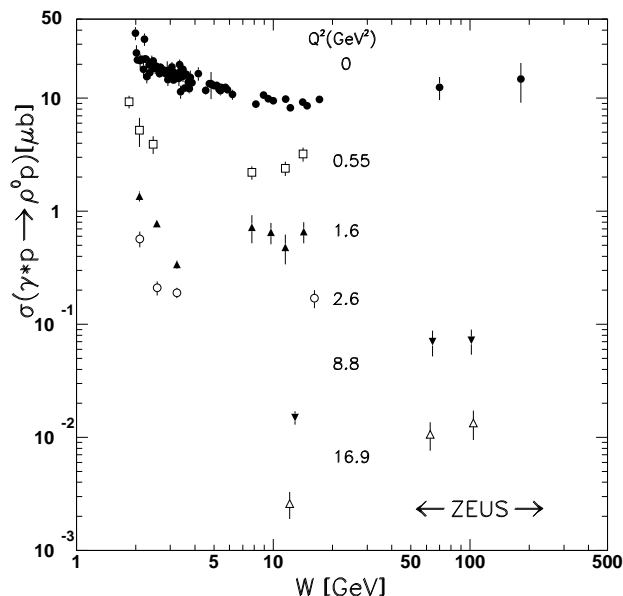


Figure 7: The  $\gamma^*p \rightarrow \rho^0 p$  cross section as a function of  $W$ , the  $\gamma^*p$  center of mass energy, for several values of  $Q^2$ . The ZEUS data at  $Q^2 = 8.8$  and  $16.9$   $\text{GeV}^2$  have an additional 31% systematic normalization uncertainty (not shown).

leads within perturbative QCD to a similar formula as the one of Donnachie and Landshoff but where, for a longitudinally polarized virtual photon at  $t = 0$ , the gluon distribution entering



the formula is that of the proton, as measured in DIS. In this case one expects the cross section to rise almost linearly with  $W$ .

The ZEUS measurements of  $\sigma(\gamma^*p \rightarrow \rho^0p)$  for photoproduction [28] and for  $7 < Q^2 < 25 \text{ GeV}^2$  and  $40 < W < 130 \text{ GeV}$  [29] are presented in figure 7 and compared with measurements at lower  $W$ . While the photoproduction cross section is slowly rising with  $W$ , that for  $Q^2 > 7 \text{ GeV}^2$  exhibits a much stronger increase relative to lower  $W$  data. In accordance with expectations the contribution of longitudinally polarized photons was found to be larger than that of the transversely polarized one (assuming  $s$  channel helicity conservation). It is interesting to note that the  $Q^2$  dependence turns out to be  $Q^{-a}$  with  $a = 4.2 \pm 0.8_{-0.5}^{+1.4}$ , again closer to the expectation of the perturbative calculations in which the increase of the gluon density with  $Q^2$  compensates partly the  $Q^{-6}$  dependence due to the two gluon exchange [30].

## 7 Conclusions

The production of large rapidity gap events in  $ep$  interactions at HERA has opened a unique opportunity to study diffractive dissociation in reactions associated with at least one hard scale, like the deep inelastic scattering or production of large transverse momenta jets. The emerging picture, if interpreted in terms of a factorizable pomeron exchange, leads to a pomeron consisting of quarks and gluons with a rather hard momentum distribution. The appearance of jets in the deep inelastic scattering and the large cross section for vector meson production measured at large  $Q^2$  and large center of mass energies could well be due to a perturbative mechanism, implying a more complicated nature of the pomeron.

## References

- [1] H1 Collab., T. Ahmed et al., Nucl. Phys. B439 (1995) 471.
- [2] ZEUS Collab., M. Derrick et al., Z. Phys. C65 (1995) 379.
- [3] ZEUS Collab., M. Derrick et al., Phys. Lett. B315 (1993) 481; Z. Phys. C68 (1995) 569.
- [4] H1 Collab., T. Ahmed et al., Nucl. Phys. B429 (1994) 477; Phys. Lett. B348 (1995) 681.
- [5] ZEUS Collab., M. Derrick et al., Phys. Lett. B346 (1995) 399.
- [6] H1 Collab., T. Ahmed et al., Nucl. Phys. B435 (1995) 3.
- [7] ZEUS Collab., M. Derrick et al., to be published; N. Pavel, DESY 95-147.
- [8] ZEUS Collab., M. Derrick et al., Phys. Lett. B332 (1995) 228.
- [9] G. Ingelman and P. Schlein, Phys. Lett. 152B (1985) 256.
- [10] A. Donnachie and P. V. Landshoff, Nucl. Phys. B244 (1984) 322.
- [11] N. N. Nikolaev and B. G. Zakharov, Z. phys. C53 (1992) 331; M. Genovese et al., KFA-IKP-TH-1994-36.
- [12] ZEUS Collab., The ZEUS Detector, Status Report 1993, DESY 1993; M. Derrick et al., Phys. Lett. B293 (1992) 465.

- [13] J. D. Bjorken, Proceedings of the 21st SLAC Summer Institute on Particle Physics, Stanford 1993 and SLAC-PUB-6463.
- [14] L. Lönnblad, *Comp. Phys. Comm.* 71 (1992) 15.
- [15] A. Donnachie and P. V. Landshoff, *Phys. Lett.* 202B (1988) 131; *Phys. Lett.* B296 (1992) 227.
- [16] A. Capella et al., *Phys. Lett.* B343 (1995) 403.
- [17] W. Buchmueller and A. Hebecker, *Phys. Lett.* B355 (1995) 573.
- [18] UA8 Collab., R. Bonino et al., *Phys. Lett.* B211(1988) 239; A. Brandt et al., *Phys. Lett.* B297 (1992) 417.
- [19] ZEUS Collab., M. Derrick et al., *Phys. Lett.* B356 (1995) 129.
- [20] L.E. Gordon and J.K. Storrow, *Z. Phys.* C56 (1992) 307.
- [21] A. Donnachie and P. V. Landshoff, *Phys. Lett.* B191 (1987) 309; *Nucl. Phys.* B303 (1988) 634.
- [22] T. Gehrman and W. J. Stirling, DTP-95-26.
- [23] H1 Collab., Julian P. Phillips, DESY 95-152C, contribution the Workshop on Deep Inelastic Scattering and QCD, Paris 1995.
- [24] P. Joos et al., *Nucl. Phys.* B113 (1976) 53; D. G. Cassel et al., *Phys. Rev.* D24 (1981) 2787; W. D. Shambroom et al., *Phys. Rev.* D26 (1982) 1.
- [25] J. Ballam et al., *Phys. Rev. Lett.* 24 (1970) 960; NMC Collab., P. Amaudruz et al., *Z. Phys.* C54 (1992) 239 and M. Arneodo et al., *Nucl. Phys.* B429 (1994) 503.
- [26] A. Donnachie and P. V. Landshoff, *Phys. Lett.* B185 (1987) 403; *Nucl. Phys.* B311 (1989); *Phys. Lett.* B348 (1995) 213.
- [27] S. J. Brodsky et al., *Phys. Rev.* D50 (1994) 3134.
- [28] ZEUS Collab., M. Derrick et al., *Z. Phys.* C63 (1994) 391; ZEUS Collab., M. Derrick et al., DESY 95-143, accepted for publication in *Z. Phys.*
- [29] ZEUS Collab., M. Derrick et al., *Phys. Lett.* B356 (1995) 601.
- [30] H. Abramowicz, L. Frankfurt and M. Strikman, DESY 95-047.